Experimental Demonstration of Conjugate-Franson Interferometry

Changchen Chen[®], Jeffrey H. Shapiro[®], and Franco N. C. Wong Research Laboratory of Electronics, Massachusetts Institute of Technology, Cambridge, Massachusetts 02139, USA

(Received 8 June 2021; accepted 4 August 2021; published 27 August 2021)

Franson interferometry is a well-known quantum measurement technique for probing photon-pair frequency correlations that is often used to certify time-energy entanglement. We demonstrate, for the first time, the complementary technique in the time basis called conjugate-Franson interferometry. It measures photon-pair arrival-time correlations, thus providing a valuable addition to the quantum toolbox. We obtain a conjugate-Franson interference visibility of $96\pm1\%$ without background subtraction for entangled photon pairs generated by spontaneous parametric down-conversion. Our measured result surpasses the quantum-classical threshold by 25 standard deviations and validates the conjugate-Franson interferometer (CFI) as an alternative method for certifying time-energy entanglement. Moreover, the CFI visibility is a function of the biphoton's joint temporal intensity, and is therefore sensitive to that state's spectral phase variation: something that is not the case for Franson interferometry or Hong-Ou-Mandel interferometry. We highlight the CFI's utility by measuring its visibilities for two different biphoton states: one without and the other with spectral phase variation, observing a 21% reduction in the CFI visibility for the latter. The CFI is potentially useful for applications in areas of photonic entanglement, quantum communications, and quantum networking.

DOI: 10.1103/PhysRevLett.127.093603

Time-energy entanglement is the quintessential quantum resource for enabling next-generation quantum technologies such as one-way quantum computation [1], quantumenhanced sensing [2-4], and quantum-secured communications [5,6]. Franson interferometry is a well-known technique for measuring the nonlocal timing coincidence of photon pairs [7]. Because Franson interference visibility resembles the Clauser-Horne-Shimony-Holt (CHSH) inequality, it is often used to characterize the quality of a biphoton's time-energy entanglement [8]. Nevertheless, Franson interferometry only quantifies the photon pair's correlation in the frequency domain and does not provide correlation information in the time domain [9]. Without time-domain characterization, Franson interferometry by itself cannot reveal a full picture of the biphoton's nonclassical correlations. Characterization of entangled photon pairs in the time domain is challenging because there is no readily available experimental method to directly measure two-photon timing correlation. One can extract two-photon time correlation from their joint temporal intensity (JTI) measurements, but they typically require sub-picosecond temporal gating and single-photon nonlinear conversion that tend to limit measurement efficiencies [10–13].

The conjugate-Franson interferometer (CFI) was proposed as a quantum measurement technique for probing two-photon correlation in the time domain, which is in contrast to the Franson interferometer's frequency-domain probing [9]. The two interferometric techniques form a complementary quantum-measurement duo for quantifying biphoton time-energy entanglement. The

Franson interferometer applies a time delay inside one arm of each of its Mach-Zehnder interferometers (MZIs) and measures coincidences to reveal frequency-domain correlations. In comparison, the conjugate-Franson interferometer applies a frequency shift inside one arm of each of its MZIs and measures frequency coincidences utilizing second-order dispersion to reveal time-domain correlations. The time-domain characterization enabled by the CFI can sense spectral phase information, and thus improve performance for a wide range of tasks that utilize high-dimensional entangled states, such as quantum communication [9], quantum sensing [14], and quantum computation [15].

Recent studies of quantum frequency combs have underscored the inability of Hong-Ou-Mandel interference (HOMI) [16] or Franson interference to distinguish two frequency combs that differ only in their spectral phase content [17]. Chang et al. argues that both HOMI and Franson interference are functions of the biphoton frequency combs's joint spectral intensity (JSI), whereas the CFI measures the state's JTI [18]. Although biphoton spectral phase information can be obtained using frequency-resolved [19] or time-resolved [20] two-photon local interference, these techniques require nearly degenerate photon pairs. The CFI, however, is a nonlocal twophoton measurement that is suitable for nondegenerate photon pairs. Other means to probe temporal correlations include the use of an electro-optic spectral shearing interferometer [21,22] with femtosecond pulse gating, as well as phase-sensitive detection with a stable and wellcharacterized classical field [23]. The CFI, on the other hand, does not require a reference field and can work with photon pairs generated by pulsed or continuous-wave (cw) pumping.

In this Letter, we report the first experimental demonstration of the CFI. We obtain a $96 \pm 1\%$ CFI fringe visibility without background subtraction for time-energy entangled photon pairs generated by cw pumped spontaneous parametric down-conversion (SPDC). Our measured visibility surpasses the quantum-classical threshold by ~ 25 standard deviations, thus validating the CFI as a valuable tool for quantifying a biphoton's time-energy entanglement. Moreover, we demonstrate the CFI's unique capability by utilizing it to distinguish between two biphoton states that differ only in their spectral phase content: one having a uniform phase, and the other with a nonuniform phase. Our CFI measurements show a visibility degradation of 21.2% for the biphoton state with a nonuniform spectral phase when compared to the visibility obtained with a uniform phase (which is transform limited), which is in agreement with our theoretical calculation. The visibility degradation indicates a decrease in timing correlation as the result of the presence of spectral phase variation whose information cannot be obtained using standard tools for analyzing the joint properties of photon pairs, such as HOMI, Franson interference, and JSI measurements [17,24,25].

The conjugate-Franson interferometer, shown in Fig. 1, comprises two MZIs that are separated in space, with each MZI having equal-length arms. For time-energy entanglement characterization, signal (idler) photons of entangled signal-idler photon pairs are sent to one (the other) MZI, and their coincidence outputs are monitored to measure the conjugate-Franson interference. An optical frequency shifter is placed in one of the arms within each interferometer, implementing a $\Delta\Omega$ frequency shift for the signal photons and a $-\Delta\Omega$ frequency shift for the idler photons, with $\Delta\Omega$ large enough to rule out single-photon interference. The frequency-shifted and the frequency-unshifted paths interfere at a 50/50 beam splitter and acquire a

phase difference of ϕ_S (ϕ_I) within the signal (idler) interferometer. The outputs from both MZIs are sent to dispersive elements that impose second-order dispersions with equal magnitudes but opposite signs. The dispersed signal and idler photons are then detected by superconducting nanowire single-photon detectors (SNSPDs), and their timing coincidences are recorded. The second-order dispersions imposed by the dispersive elements correlate the frequency content of the inputs to their measured arrival times, thus effectively converting the performed timedomain measurement result to a frequency-domain measurement. The opposite signs of the two dispersive elements together with nonlocal dispersion cancellation [6,26] recover the signal-idler frequency coincidences as signalidler timing coincidences, and thus distinguish between different signal-idler sum frequencies.

The biphoton for time-energy entangled photon pairs produced by cw pumped SPDC can be written in its time-domain representation as [27]

$$|\psi\rangle_{\rm SI} \propto \int \mathrm{d}t_- \psi_{\rm SI}(t_-)|t_+ + t_-/2\rangle_S |t_+ - t_-/2\rangle_{\rm I}, \quad (1)$$

where $t_+ = (t_{\rm S} + t_{\rm I})/2$ and $t_- = (t_{\rm S} - t_{\rm I})$, with $t_{\rm S}$ ($t_{\rm I}$) representing the time for the signal (idler) photon. $\psi_{\rm SI}(t_-)$ is the joint temporal amplitude, and its magnitude squared is the joint temporal intensity ${\rm JTI}(t_-) = |\psi_{\rm SI}(t_-)|^2$. The CFI's coincidence probability is given by [27]

$$P_{\text{CFI}}(\phi_T) = \frac{\eta^2}{8} \left(1 + \int dt_{\text{-}} JTI(t_{\text{-}}) \cos(\Delta \Omega t_{\text{-}} + \phi_T) \right), (2)$$

where $\phi_T = \phi_S + \phi_I$ is the sum of the signal and idler MZI phase differences in the CFI, and η is the measurement efficiency in each MZI. The resulting visibility is

$$V_{\text{CFI}} = \int dt_{-} \text{JTI}(t_{-}) \cos(\Delta \Omega t_{-}). \tag{3}$$

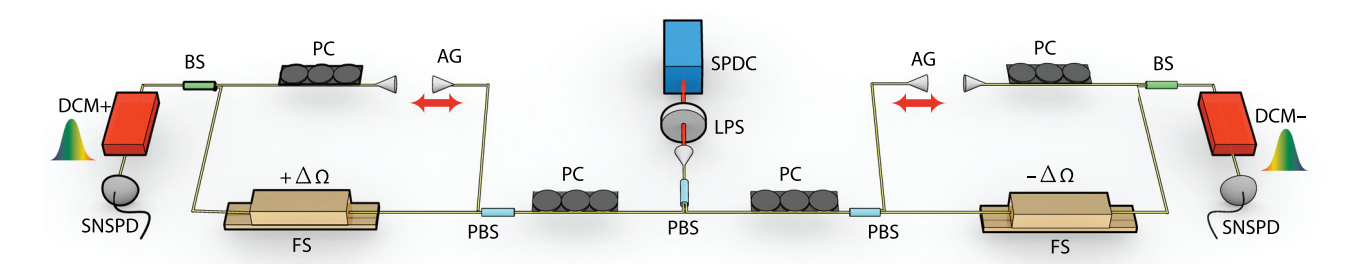


FIG. 1. Experimental setup of our conjugate-Franson interferometer. Time-energy entangled signal-idler photon pairs generated by cw pumped SPDC were coupled into an optical fiber and routed to their respective MZIs. The signal's frequency shifter was configured to blue shift its input, whereas the idler's shifter was configured to red shift its input. The polarization and the path lengths between the two arms of each MZI were made to be the same. The fiber-based CFI was placed inside a custom-built two-stage thermal box for phase stabilization. The MZI outputs were detected with SNSPDs, and their arrival times were recorded for coincidence measurements. LPS: long-pass filter; PBS: polarizing beam splitter; PC: polarization controller; FS: frequency shifter for $\Delta\Omega$ ($-\Delta\Omega$) frequency shift; AG: tunable air gap; BS: 50/50 beam splitter; and DCM + (-): dispersion module with normal (anomalous) dispersion.

This visibility result is similar to those obtained in Franson interferometry for time-energy entangled photons [7] and the CHSH test with polarization-entangled photons [8], in that the CFI is in the same class of quantum measurements for testing the violation of local hidden-variable theory and quantifying the nonlocal feature of entanglement.

To demonstrate conjugate-Franson interferometry, we built a CFI as shown in the experimental schematic of Fig. 1 with inputs of time-energy entangled photon pairs generated from SPDC in a type-II phase-matched periodically poled potassium titanyl phosphate waveguide pumped by a 780 nm cw laser. The orthogonally polarized signal and idler photons were nondegenerate with ~200 GHz offset between their center frequencies, and each had a full width at half-maximum bandwidth of 320 GHz. The photon pairs were separated using a fiber polarizing beam splitter and sent to their respective MZIs. We repurposed two dualdrive quadrature phase-shift keying modulators (Fujitsu FTM7961EX) operating in a configuration for single sideband generation as the frequency shifters and set the frequency shift at $\pm \Delta\Omega/2\pi = \pm 15.65$ GHz [28]. We first characterized the frequency-shifted outputs from both frequency shifters using a narrow-band cw laser at 1560 nm, as shown in Fig. 2(a). Within the desired frequency range from $-\Delta\Omega$ to $\Delta\Omega$, a carrier-to-sideband

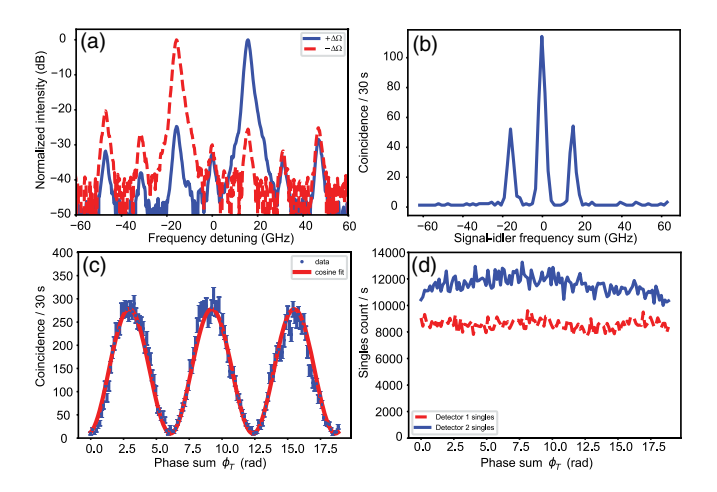


FIG. 2. (a) Log-scale display of frequency shifters' output spectra, measured using classical light, that shows signal-to-noise ratios of at least 20 dB limited by higher-order sidebands. Maximum intensities of both spectra normalized to 0 dB. (b) Measured CFI coincidences vs inferred signal-idler frequency sum: central peak location determines zero detuning of signal-idler sum frequency. Thirty-second integration time for each data point; measurement taken with MZI phase sum of $\phi_T \approx \pi/2$. (c) Coincidences (blue) as a function of MZI phase sum ϕ_T , with calculated uncertainties assuming Poisson statistics. Least-squares fit (solid red line) to the form $A[1 + V\cos(\phi_T)]$ yields a fitted CFI visibility V of 93%. No background counts are subtracted from measured data. (d) Singles count rates for both detectors as functions of MZI phase sum ϕ_T , showing no meaningful variations.

ratio of at least 25 dB was achieved for both blue and red frequency shifters. During operation, the signal's MZI had an 18.6 dB insertion loss and the idler's MZI had a 22.7 dB insertion loss. These high insertion losses were mainly due to the low conversion efficiencies of the frequency shifters [28]. The different insertion losses of the two MZIs were caused by performance differences of the two frequency shifters and tunable air gaps. The outputs from the signal and idler MZIs were sent to fiber Bragg-grating dispersion modules that imposed equal magnitude but opposite sign dispersions of ± 10 ns/nm. These dispersion modules had 3 dB insertion loss and a passband from 1557.85 nm (192.44 THz) to 1563.05 nm (191.80 THz). The photons emerging from the dispersion modules were detected using tungsten silicide SNSPDs with ~80% system efficiency and a 120 ps timing jitter. The detected signal and idler spectral ranges were limited by the dispersion modules' 640 GHz passband. The detection events were time tagged using a time tagger (Hydraharp 400) with a 128 ps timing resolution.

Because the SPDC signal-idler photon pairs are timeenergy entangled, the imposed opposite dispersions cancel and their arrival times remain correlated. Nevertheless, the existence of dispersion reveals the incoming photons' frequency information. The resolution of our frequencydomain measurement is 1.8 GHz, which is determined by the detectors' timing jitters and the amount of applied dispersions. A sample signal-idler coincidence measurement from the CFI is shown in Fig. 2(b). The locations of the coincidence peaks correspond to the signal-idler sum frequencies, which in turn indicate the possible paths the signal and idler photon have traveled. The two side peaks correspond to cases in which only one of the signal and idler photons has been frequency shifted such that the signal-idler frequency sum is detuned by $\pm \Delta\Omega/2\pi = \pm 15.65$ GHz. For the center peak, the sum frequency remains unchanged, requiring that both photons travel along their frequencyunshifted arms or they both go through their respective frequency shifters. The two different paths are indistinguishable, and they interfere as a function of the MZI phase sum ϕ_T , producing the CFI's nonlocal coincidence interference similar to that of the Franson interferometer. We note that if the dispersion modules were not present, the three peaks could not be separated and the maximum interference visibility achievable would be limited to 50%, which is inadequate to distinguish a quantum (nonclassical) state from a classical state.

We observed that the strength of the center coincidence peak varied as a function of the phase sum ϕ_T . The CFI was thermally insulated. In particular, we found that the center coincidence peak changed its magnitude due to residual thermal drift at an estimated rate of 0.29 ± 0.06 rad/min for ϕ_T . We recorded the signal-idler coincidences and plotted the coincidence counts of the center peak against the estimated accumulated phase sum ϕ_T , as shown in

Fig. 2(c). The result shows a clear oscillatory signature as a function of the phase drift. To eliminate the possibility that the change of the coincidence counts was caused by changes of the photon flux, we also recorded the singles rates of both detectors at the same time during the coincidence measurement, as shown in Fig. 2(d). The measured singles rates remain constant throughout the thermal drift's duration and show that the oscillatory fringe is not a result of single-photon interference.

To obtain an accurate value for the CFI's interference visibility, we attached a piezoelectric transducer stack to the signal MZI's frequency-unshifted arm as a fiber stretcher to impose a controllable phase shift on ϕ_S . We repeatedly scanned $\phi_{\rm S}$ from 0 to 2π while keeping $\phi_{\rm I}$ constant. The fringe visibility was calculated based on the observed minimum and maximum coincidence counts within each phase scan [27]. We obtain a CFI visibility of $96 \pm 1\%$ based on 23 phase-scan measurements and an uncertainty of one standard deviation. We estimate that degradation of our CFI visibility measurements was due to phase fluctuations of the CFI (1.2%), the modulators' extra sidebands (0.7%), modulator dispersion (0.5%), dark counts and noise background (0.5%), and SPDC multipair events (0.4%). The achieved visibility validates the quantum nonlocal correlation between our SPDC photon pairs, surpassing the quantum-classical threshold of $1/\sqrt{2} = 70.7\%$ by ~ 25 standard deviations. This high CFI visibility confirms that our photon-pair source indeed produces time-energy entanglement and validates conjugate-Franson interferometry being a promising quantum-measurement technique for certifying time-energy entanglement. We note that although our current measurement setup is affected by the postselection loophole, it can be modified to match the two side peaks temporally and eliminate the postselection loophole [29].

To demonstrate that the CFI visibility is sensitive to the spectral phase of a biphoton state, we first consider a cw pumped SPDC source generating a time-energy entangled biphoton state with a flat spectrum spanning 320 GHz and no spectral phase variation; i.e., its frequency-domain description is

$$|\psi^{(1)}\rangle_{\mathrm{SI}} \propto \int_{-\omega_{\mathrm{max}}}^{\omega_{\mathrm{max}}} \mathrm{d}\omega \Psi_{\mathrm{SI}}^{(1)}(\omega) |\omega_{\mathrm{S}_0} + \omega\rangle_{\mathrm{S}} |\omega_{\mathrm{I}_0} - \omega\rangle_{\mathrm{I}}, \quad (4)$$

where $\Psi_{\rm SI}^{(1)}(\omega)=1/\sqrt{2\omega_{\rm max}}$ is its joint spectral amplitude (JSA), $\omega_{\rm S_0}$ ($\omega_{\rm I_0}$) is the signal (idler) center frequency, and ω is the state's frequency detuning with a range of $\pm\omega_{\rm max}$, where $\omega_{\rm max}/2\pi=160$ GHz. Now, consider the state $|\psi^{(2)}\rangle_{\rm SI}$ whose JSA is

$$\Psi_{\rm SI}^{(2)}(\omega) = \begin{cases} 1/\sqrt{2\omega_{\rm max}}, & \text{for } |\omega| \le \omega_1\\ e^{i\phi}/\sqrt{2\omega_{\rm max}}, & \text{for } \omega_1 < |\omega| \le \omega_{\rm max}, \end{cases}$$
 (5)

where $\omega_1/2\pi = 80$ GHz.

Although $|\psi^{(2)}\rangle_{SI}$ differs from $|\psi^{(1)}\rangle_{SI}$ when $0 < \phi < 2\pi$, these states cannot be distinguished by Franson or Hong-Ou-Mandel interference because $|\psi^{(2)}\rangle_{SI}$ and $|\psi^{(1)}\rangle_{SI}$ have identical JSIs, as shown in Fig. 3(a), and those interferometers' interference patterns are determined by the JSI. On the other hand, the JTIs of $|\psi^{(2)}\rangle_{SI}$ and $|\psi^{(1)}\rangle_{SI}$ are different because of the JTI's spectral phase dependence. This difference is shown in Figs. 3(b) and 3(c), which display the JTIs of $|\psi^{(2)}\rangle_{SI}$ for $\phi=0$ and π , respectively, with the former also being the JTI of $|\psi^{(1)}\rangle_{SI}$. Equation (3) indicates that the CFI visibility is a function of the JTI, and thus sensitive to spectral phase. Our theoretical calculation for the CFI visibility yields 95.1% for $|\psi^{(1)}\rangle_{SI}$ and 75.5% for $|\psi^{(2)}\rangle_{SI}$ with $\phi=\pi$. This represents an \sim 20% drop in CFI visibility that should be measurable experimentally.

We used a type-0 phase-matched periodically poled lithium niobate crystal pumped by a 780 nm cw laser to generate time-energy entangled photon pairs with a few terahertz of bandwidth. A 50/50 beam splitter was used to separate the copolarized signal and idler photons that incurred a 3 dB loss for postselected signal-idler coincidence measurements. We applied a programmable amplitude and phase spectral filter (Finisar WaveShaper 1000S) to shape the signal and idler spectra to be rectangular with a 320 GHz flat bandwidth and to impose an adjustable phase $e^{i\phi}$ on both signal and idler light for frequency detuning of $|\omega|/2\pi$ between 80 and 160 GHz, thus producing the biphoton state $|\psi^{(2)}\rangle_{SI}$. We measured the CFI visibility at $\phi = 0, \pi/2, \pi, 3\pi/2$, and 2π ; and Fig. 4 displays our results along with the theoretically calculated values. Because $\phi=0$ or 2π makes $|\psi^{(2)}\rangle_{\rm SI}=|\psi^{(1)}\rangle_{\rm SI}$, the $93.2\pm2.0\%$ visibility we obtained for $\phi=0$ and the $91.4\pm2.0\%$ we

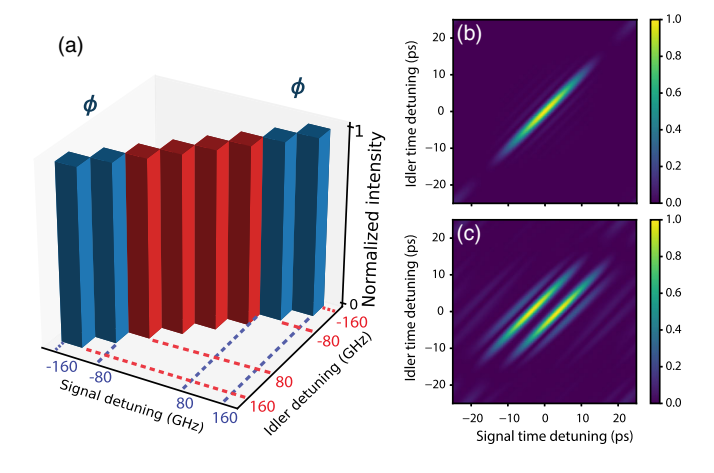


FIG. 3. (a) JSI calculated for a biphoton with 320-GHz-wide flat-top spectrum. Spectral phase ϕ (none, set to zero) applied to blue (red) shaded region outside (within) the ± 80 GHz span of signal and idler frequency detuning. JSI does not depend on ϕ . (b) JTI of same biphoton state with $\phi = 0$ or 2π . (c) JTI of same biphoton state with $\phi = \pi$. Maximum of JTI normalized to one.

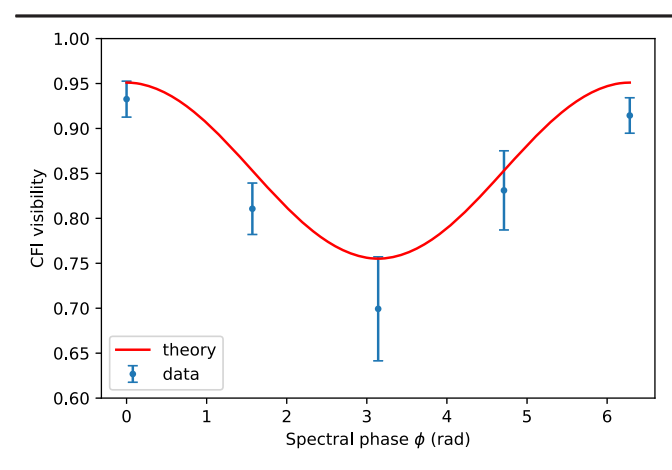


FIG. 4. Conjugate-Franson fringe visibility as a function of applied spectral phase ϕ of Eq. (5). Measured data points (blue) closely follow calculated values (solid red line) obtained from Eq. (3), with a rectangular spectrum of 320 GHz span shown in Fig. 3(a). Error bars represent one standard deviation of three measurements.

got for $\phi=2\pi$, with the uncertainty value being the standard deviation of three measurements, are consistent with that equivalence. Figure 4 shows that the CFI visibility degrades when spectral phase variation is introduced, reaching a minimum visibility of $72.0\pm3.1\%$ for $\phi=\pi$, which is in good agreement with our calculation. In this simple example, the substantial visibility reduction of 21.2% from $\phi=0$ to $\phi=\pi$ clearly confirms the ability of the CFI to distinguish between states with different spectral phase content.

In summary, we reported the first experimental realization of the conjugate-Franson interferometer, demonstrating a CFI visibility of $96 \pm 1\%$ without any background subtraction for time-energy entangled photon pairs generated by cw pumped SPDC. The achieved visibility surpasses the quantum-classical threshold of ~71% by 25 standard deviations and clearly validates the quantum entanglement feature between the SPDC signal and idler photons. To illustrate its application potential, we utilized the CFI as an enabling quantum-measurement technique to distinguish between two biphoton states with identical joint spectral intensities but different joint temporal intensities due to spectral phase variation. By introducing an adjustable spectral phase shift to a cw pumped SPDC biphoton state, we observed a significant CFI visibility drop of 21% between the two biphoton states, matching our theoretical calculations. Our results show that conjugate-Franson interferometry quantifies correlation in the time domain and is complementary to the well-known Franson interferometry. Overall, we expect that the addition of the CFI to the quantum toolbox provides a simpler way to characterize time-domain correlation and a new method to monitor spectral phase information of time-energy entangled photon pairs. Hence, we believe the CFI will enhance future developments of entanglement systems for computing, communication, and sensing applications.

This work was supported by the National Science Foundation under Grant No. 1741707. The authors thank Catherine Lee and Dirk Englund for providing the Proximion dispersion compensation modules, and Boya Ye for generating the experimental schematic.

- chencc@mit.edu
- [1] M. A. Nielsen, Phys. Rev. Lett. 93, 040503 (2004).
- [2] Z. Zhang, S. Mouradian, F. N. C. Wong, and J. H. Shapiro, Phys. Rev. Lett. 114, 110506 (2015).
- [3] S. Lloyd, Science **321**, 1463 (2008).
- [4] Y. Zhang, D. England, A. Nomerotski, P. Svihra, S. Ferrante, P. Hockett, and B. Sussman, Phys. Rev. A 101, 053808 (2020).
- [5] T. Zhong et al., New J. Phys. 17, 022002 (2015).
- [6] C. Lee, Z. Zhang, G. R. Steinbrecher, H. Zhou, J. Mower et al., Phys. Rev. A 90, 062331 (2014).
- [7] J. D. Franson, Phys. Rev. Lett. **62**, 2205 (1989).
- [8] J. F. Clauser, M. A. Horne, A. Shimony, and R. A. Holt, Phys. Rev. Lett. 23, 880 (1969).
- [9] Z. Zhang, J. Mower, D. Englund, F. N. C. Wong, and J. H. Shapiro, Phys. Rev. Lett. 112, 120506 (2014).
- [10] A. Pe'er, B. Dayan, A. A. Friesem, and Y. Silberberg, Phys. Rev. Lett. 94, 073601 (2005).
- [11] O. Kuzucu, F. N. C. Wong, S. Kurimura, and S. Tovstonog, Phys. Rev. Lett. 101, 153602 (2008).
- [12] S. Mittal, V. V. Orre, A. Restelli, R. Salem, E. A. Goldschmidt, and M. Hafezi, Phys. Rev. A 96, 043807 (2017).
- [13] J.-P. W. MacLean, J. M. Donohue, and K. J. Resch, Phys. Rev. Lett. 120, 053601 (2018).
- [14] M. G. Raymer, A. H. Marcus, J. R. Widom, and D. L. P. Vitullo, J. Phys. Chem. B 117, 15559 (2013).
- [15] C. Reimer et al., Nat. Phys. 15, 148 (2019).
- [16] C. K. Hong, Z. Y. Ou, and L. Mandel, Phys. Rev. Lett. 59, 2044 (1987).
- [17] N. B. Lingaraju, H. Lu, S. Seshadri, P. Imany, D. E. Leaird, J. M. Lukens, and A. M. Weiner, Opt. Express 27, 38683 (2019).
- [18] K. Chang et al., npj Quantum Inf. 7, 48 (2021).
- [19] N. Tischler, A. Büse, L. G. Helt, M. L. Juan, N. Piro, J. Ghosh, M. J. Steel, and G. Molina-Terriza, Phys. Rev. Lett. 115, 193602 (2015).
- [20] P. Chen, C. Shu, X. Guo, M. M. T. Loy, and S. Du, Phys. Rev. Lett. **114**, 010401 (2015).
- [21] A. O. C. Davis, V. Thiel, M. Karpiński, and B. J. Smith, Phys. Rev. Lett. 121, 083602 (2018).
- [22] A. O. C. Davis, V. Thiel, and B. J. Smith, Optica 7, 1317 (2020).
- [23] F. A. Beduini, J. A. Zielińska, V. G. Lucivero, Y. A. de Icaza Astiz, and M. W. Mitchell, Phys. Rev. Lett. 113, 183602 (2014).
- [24] C. Chen, C. Bo, M. Y. Niu, F. Xu, Z. Zhang, J. H. Shapiro, and F. N. C. Wong, Opt. Express **25**, 7300 (2017).

- [25] K. Zielnicki, K. Garay-Palmett, D. Cruz-Delgado, H. Cruz-Ramirez, M. F. OBoyle, B. Fang, V. O. Lorenz, A. B. U'Ren, and P. G. Kwiat, J. Mod. Opt. 65, 1141 (2018).
- [26] J. D. Franson, Phys. Rev. A 45, 3126 (1992).
- [27] See Supplemental Material at http://link.aps.org/supplemental/10.1103/PhysRevLett.127.093603 for details
- on the CFI's coincidence-count behavior and the experimental setup.
- [28] C. Chen, J. E. Heyes, J. H. Shapiro, and F. N. C. Wong, Sci. Rep. 11, 300 (2021).
- [29] F. Vedovato, C. Agnesi, M. Tomasin, M. Avesani, J. A. Larsson, G. Vallone, and P. Villoresi, Phys. Rev. Lett. **121**, 190401 (2018).